



Investigation of Compressive Behavior of Pre-folded Thin-walled Column Fabricated by 3D Printing

Farid Triawan^{1,*}, Elin Rachmawati^{1,2}, Bentang Arief Budiman³, Djati Wibowo Djamari¹, Andy Saputro³, Ilman Arpi³

¹Department of Mechanical Engineering, Sampoerna University, Jl. Raya Pasar Minggu 16, Jakarta, Indonesia.

²Department of Aerospace and Mechanical Engineering, The University of Arizona, Tucson, AZ, 85721, US.

³Faculty of Mechanical and Aerospace Engineering, Institut Teknologi Bandung, Jl. Ganesha 10, Bandung, Indonesia

Correspondence: E-mail: farid.triawan@sampoernauniversity.ac.id

ABSTRACT

This paper reveals the mechanical behavior of thin-walled columns with pre-folded patterns subjected to compressive loading. The column specimens (Polylactic Acid) are fabricated using Fused Deposition Modeling 3D printer and subjected to quasi-static compressive loading to investigate their mechanical behavior (by modifying the specimens' cross-section patterns and folding angles). The column specimens are simulated by finite element analysis to understand how the stress distribution and local deformation affecting the stiffness, strength, and overall deformation. The experiments showed that introducing the pre-folded pattern in a thin-walled column with different cross-sections can dramatically lower its structural stiffness (85%) and compressive strength (69%), but increase its deformability (115%), which is good agreement with numerical simulation. The variation of cross-section patterns and pre-folding angle could effectively modify the compressive mechanical behavior. Moreover, the results demonstrate how the FDM 3D Printing method can be used in fabricating a thin-walled column with irregular shapes and then to modify its deformability. This finding can be useful for designing any complex structures requiring specific stiffness and deformation such as suspension devices, prosthetic devices in biomechanics, and robotic structures.

ARTICLE INFO

Article History:

Submitted/Received 13 May 2021

First revised 01 Jul 2021

Accepted 26 Sep 2021

First available online 27 Sep 2021

Publication date 01 Dec 2021

Keyword:

3D printing,

Deformability,

Engineering

Polylactic acid (PLA),

Pre-folded thin-walled column,

Structural stiffness.

1. INTRODUCTION

Thin-walled columns have been studied and used in many engineering applications for years because of their excellent mechanical properties and behavior (Daneshi & Hosseinipour, 2002; Gholipour *et al.*, 2018; Lee *et al.*, 1999; Ma & You, 2014a; Moon *et al.*, 2014; Nia & Hamedani, 2010; Reid, 1993; Singace & El-Sobky, 1997; Triawan *et al.*, 2020; Wang *et al.*, 2016). The columns are prominent for structural applications, such as in buildings (Ma & You, 2014a; Wang *et al.*, 2016), vehicles (Triawan *et al.*, 2020), aircraft (Moon *et al.*, 2014), and ships (Gholipour *et al.*, 2018). It is often used as the load-bearing component; thus, it is mostly operated under compressive mode with some possible structural modification such as those of corrugated tubes (Nia & Hamedani, 2010; Singace & El-Sobky, 1997; Triawan *et al.*, 2020), aluminum tubes for space frame (Lee *et al.*, 1999), and metal thin-walled tube for vehicle crashworthiness (Daneshi & Hosseinipour, 2002; Reid, 1993).

Among these thin-walled column applications, the usage of a column with a pre-folded pattern has received remarkable attention due to its flexibility in the mechanical properties and behavior, which can be adjusted following the design requirements (Han & Park, 1999). These columns typically consist of folded sheets or intricate modules, and they exhibit some unique characteristics, such as auxetics, tunable nonlinear stiffness, and multi-stability. Many scholars have applied the pre-folded approach to absorb energy for crashworthiness design (Yang *et al.*, 2016, 2018). A typical design approach to enhance a vehicle's crashworthiness is to install energy absorption devices that deform and absorb kinetic energy during a low-speed collision (Ma & You, 2014b). Both experimental and numerical results show that the pre-folded pattern develops a diamond-shaped mode, reducing initial peak force and a significant increase in energy

absorption compared to the conventional hexagonal tube (Ma *et al.*, 2019). The elevated overall force level, in turn, increases the total energy absorbed. These unique advantages are highly desirable traits for energy absorption devices (Chen *et al.*, 2019). A successfully designed energy absorber must exhibit three key benefits: low peak load, controllable deformation mode, and high energy absorption efficiency (Triawan *et al.*, 2020; Zhou *et al.*, 2021).

Most of the research discussion on pre-folded thin-walled columns is mainly focusing on plastic deformation to absorb the kinetic energy only. Meanwhile, as load-bearing structures or suspension devices, the mechanical behavior of pre-folded thin-walled columns in the elastic region is a major concern that should be revealed. For example, a column with a pre-folded pattern could be used for suspension components of a building or bridge, which enables avoiding damage caused by vibrational energy excitation coming from earthquakes or wind (Ishida *et al.*, 2017; Nikoo *et al.*, 2020). In biomechanics application, the pre-folded thin-walled column could be used for biomedical stents (Kuribayashi *et al.*, 2006) and suspension for prosthetic devices (Sadeghi & Li, 2019). Furthermore, the column is also suitable for suspension components in robotic structures, which usually have complex structures and irregular shapes (Castiblanco *et al.*, 2021; Yu *et al.*, 2020). All these applications utilize the elastic mechanical properties and behavior of the column and do not allow any plastic deformation to avoid failure. However, there is only limited study that investigates the elastic behavior of the pre-folded thin-walled columns. The relationship between the column's geometry and its mechanical behavior, especially in the elastic region, is a challenging issue that has not been well explored (Al-Kaseasebh & Mamaghani, 2019).

This study reveals the compressive behavior of pre-folded thin-walled columns,

especially in the elastic region, as it is essential for suspension devices. A Fused Deposition Modeling (FDM) 3D printer is used to fabricate the column specimens made of Polylactic Acid (PLA) material. The FDM 3D printing method is chosen because it has several advantages in developing the thin-walled column specimens, including low cost, easy operation, and rapid fabrication of irregular-pattern products (Hadisujoto & Wijaya, 2021; Triawan *et al.*, 2020). The column specimens with three kinds of cross-sections and five different pre-folded angles are prepared for the compression test experiment. The measured stress and strain curves are used to analyze the stiffness, strength, and deformation behavior. Subsequently, finite element analysis on the column models is performed to clarify the mechanical behavior. The comparison result between experiment and simulation is then discussed to reveal the effects of pre-folded angle and cross-section patterns on the compressive behavior.

2. METHODS

2.1. Design and Fabrication of Pre-Folded Thin-Walled Column

Table 1 shows the PLA mechanical properties (Rismalia *et al.*, 2019). The 3D printed specimen of PLA materials demonstrates a brittle failure.

Figure 1(a) shows the geometry of the pre-folded thin-walled column model. The structure's total height is set as 125 mm with wall thickness, and the cross-section area (A) is 0.8 mm and 1800 mm², respectively. The cross-section is varied with 3 shapes which are triangular (TRI), square (SQU), and

hexagonal (HEX). The height is divided into five stacking layers of which the angle ϑ is varied with 5 different values of 140, 150, 160, 170, and 180° (non-folded column). **Figure 1(b)** shows the cross-section shapes with identical total areas but different side lengths (l). The side length l of the hexagonal, square, and triangular cross-sections can be calculated using Equations [1], [2], and [3], respectively. From the calculation, the triangular l was 64.5 mm, square l was 42.4 mm, and hexagonal l was 26.3 mm.

$$l = \sqrt{\frac{A}{\frac{3}{2} \sqrt{3}}} \quad (1)$$

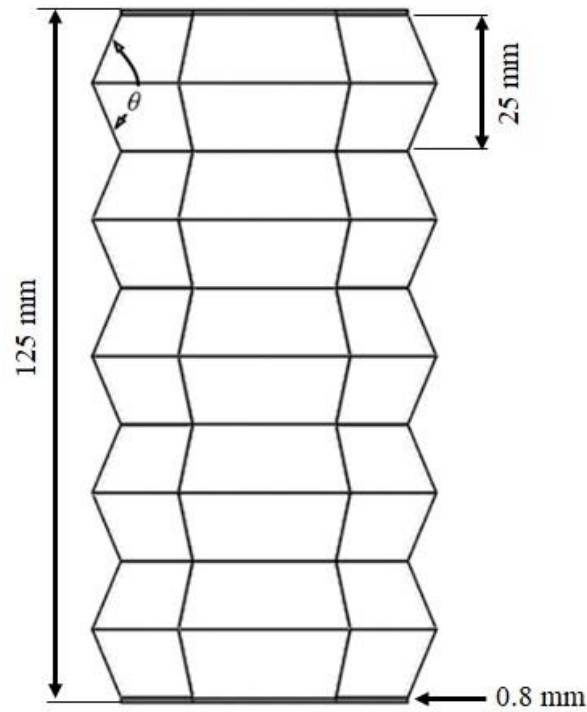
$$l = \sqrt{A} \quad (2)$$

$$l = \sqrt{\frac{A}{\frac{1}{4} \sqrt{3}}} \quad (3)$$

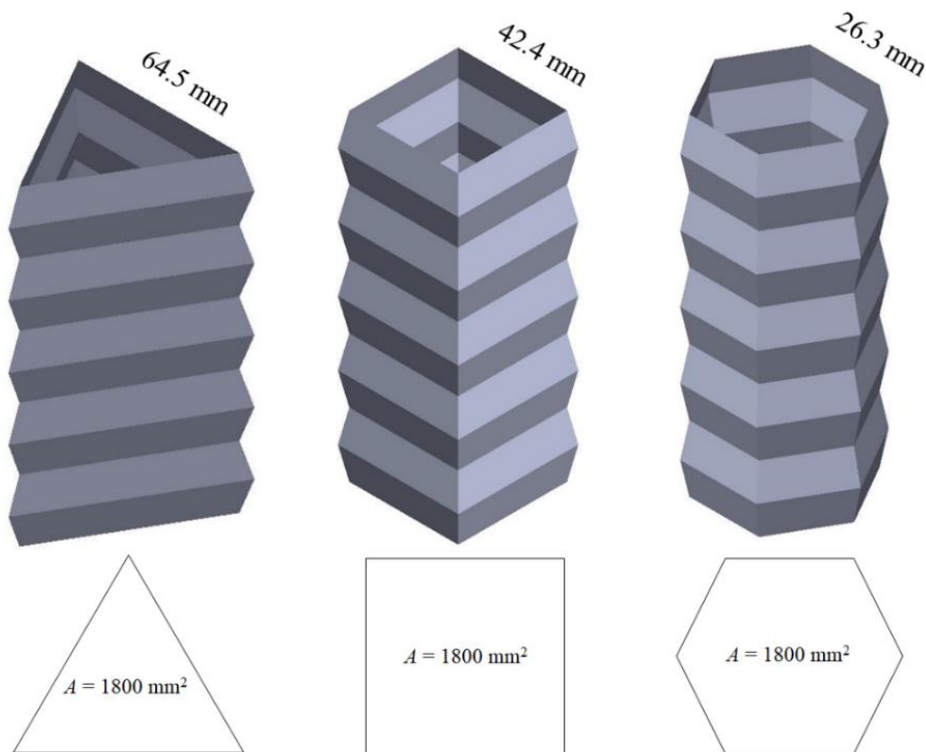
The pre-folded thin-walled column was fabricated using the Fused Deposition Modeling (FDM) 3D printing method. Firstly, the design from Solidworks software (.SLDPRT or .SLDASM) was converted into a supported file for the 3D printer software (g.code or .STL file) by Ultimaker Cura 3.6.0 software. The input in Ultimaker Cura 3.6.0 was then used to set up the printing configuration. ANYCUBIC I3 Mega 3D printer was used to manufacture the column specimens, and the printing filament is Polylactic Acid (PLA) with a diameter of 1.75 mm. The infill pattern was set as a Lines pattern with 90° crossing to each other path. The infill density of the lines pattern was set to be 25%.

Table 1. PLA mechanical properties (Rismalia *et al.*, 2019).

Properties	Values
Infill Pattern	Lines
Infill density	25%
Elastic modulus	2.76 GPa
Tensile strength	29.7 MPa



(a)



(b)

Figure 1. The geometry of pre-folded thin-walled column (a) in 2-dimensional view and (b) section shape variations of a pre-folded thin-walled column. From left to right: triangular, square, and hexagonal. The cross-section column area (A) of each shape is maintained constant i.e., 1800 mm^2 .

2.2. Compressive Test Procedure

The compressive test was performed for all specimens under quasi-static axial loading. Test Resource 313 Universal Testing Machine was used for the compression test. The compression rate is 1.0 mm/min and set to stop when the specimens fractured. This compression rate refers to ASTM D695 as the standard test method for compressive properties of rigid plastics. During the test, the lower and upper jig are greased to minimize friction forces during compression. The experimental setup of the compression test is shown in **Figure 2**.

From the compression test, the force and displacement data were acquired and then plotted. The column structural stiffness (k) was calculated from the slope of the force (F) – displacement (δ) curves as shown in Equation [4].

$$k = \frac{dF(\delta)}{d\delta} \quad (4)$$

Furthermore, the pre-folded column strength under compressive loading (S_{com}) is defined as the maximum force that can be held by the specimens when being compressed before the material is broken. The S_{com} can be calculated by dividing maximum force (F_M) with cross-section column area (A) as shown in Equation [5].

$$S_{com} = \frac{F_M}{A} \quad (5)$$

2.3. Finite Element Analysis (FEA)

Numerical simulation by FEA was conducted using Abaqus 2020 software to investigate the stress and strain distributions in the column. The force applied to the structure leads to failure when the stress level exceeds the PLA tensile strength. The numerical simulation also provides a better understanding of the critical location of the stress distribution along with the structure. Using simulation, deformation in the edge and wall can also be observed further.

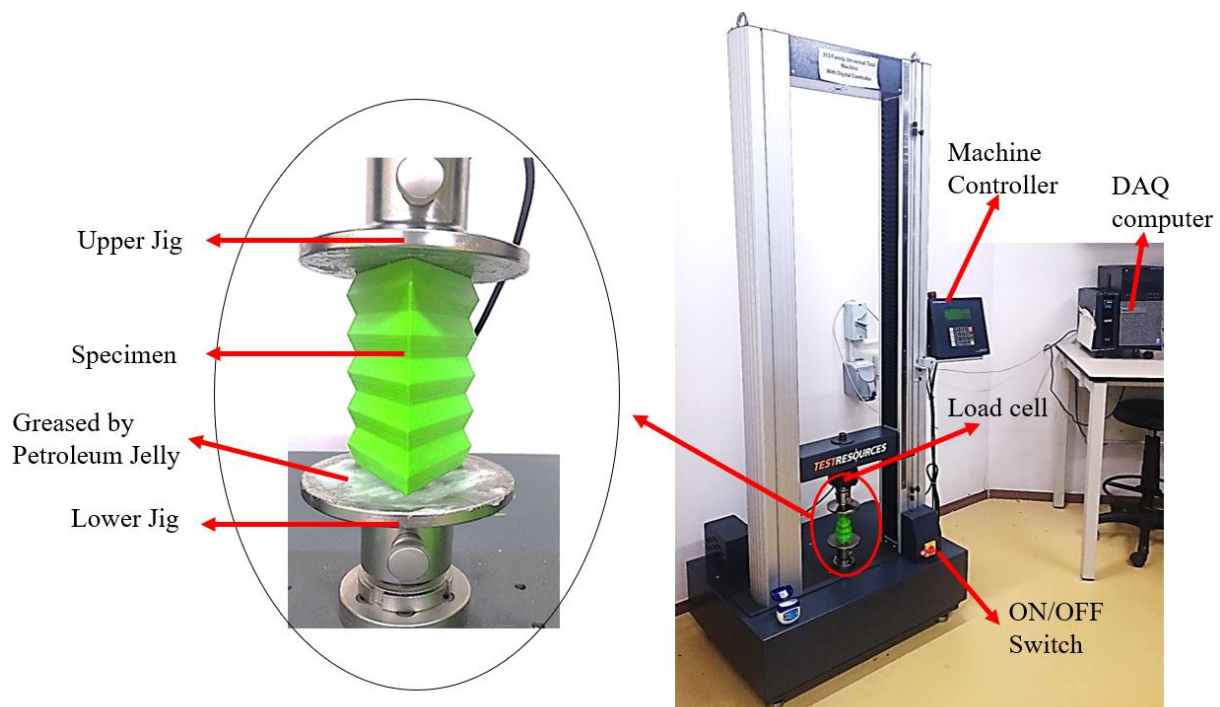


Figure 2. Experimental setup of compression test.

Meshing was conducted for each shape model with element type and size of triangular and 0.5 mm, respectively. Total meshing elements for triangular shape column was 28080 elements, for square shape column was 24440 elements, and for hexagonal shape, the column was 22620 elements. These element sizes and numbers are sufficient to assure the obtained stress and deformation are independent of them. The details for each column meshing condition are shown in **Figure 3**.

After the meshing process, the boundary condition was applied to mimic the experimental compression test. Fixed support, which is zero displacements ($\delta_x, \delta_y, \delta_z$) in the x -axis, y -axis, and z -axis, was applied at one point of the bottom surface as indicated in **Figure 4**. Furthermore, zero displacement in z -axis (δ_z) for other points at the bottom column was also applied

to assure no torsion displacement occurs during simulation. Uniform displacement indicated by the downward arrow was then applied at the top points of the structure in a negative z -axis direction.

The FEA of the columns with a large deformation effect was implemented by activating the nonlinear behavior (NLGEOM function), respectively. The specimen failure considerably occurs if any local region on the column has reached a condition in which the maximum principal stress is over the tensile strength of the PLA material. The maximum principal stress (σ_1) is used as the failure criterion since, in the tensile test result, the PLA material fails in brittle behavior (Rismalia et al., 2019). Note that at this state, the F_M and δ_y values of each simulation case were recorded. The k and S_{com} of simulation were then calculated by using Equations [3] and [4].

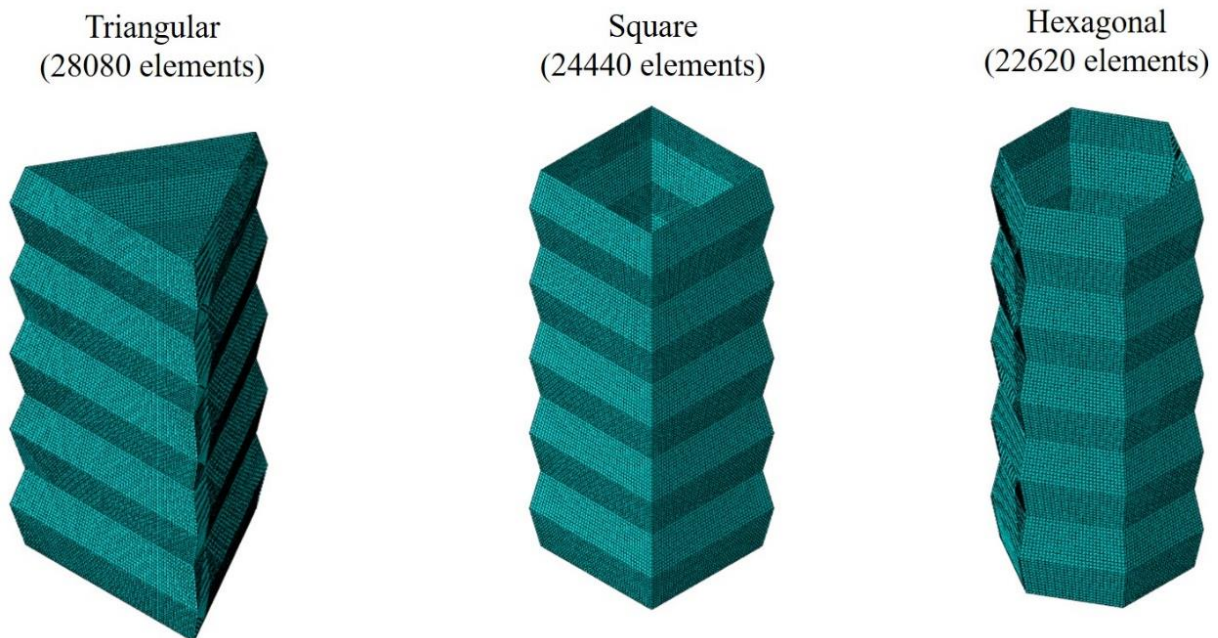


Figure 3. Meshing condition for each cross-section shape pre-folded thin-walled column.

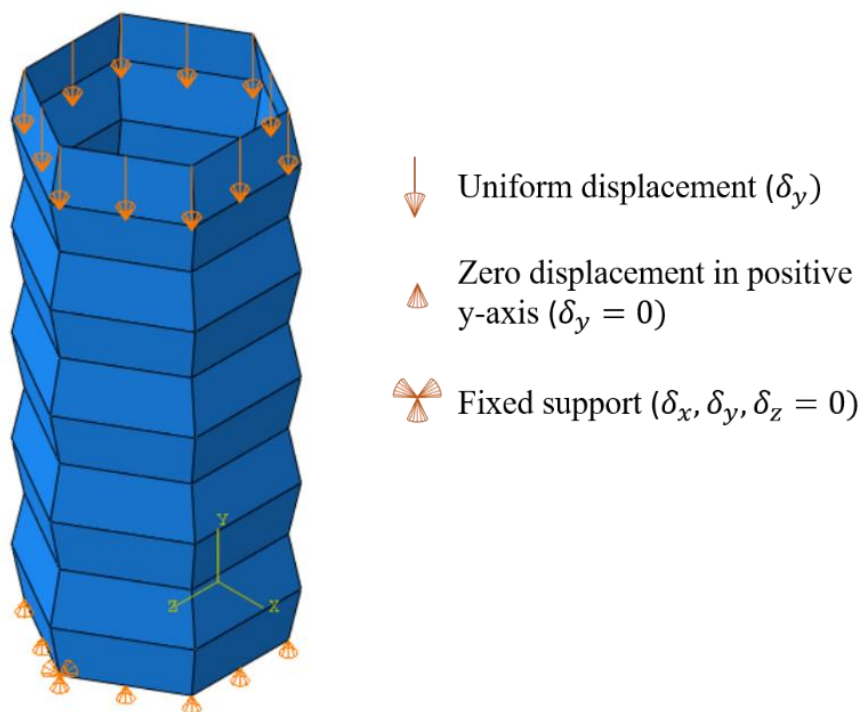


Figure 4. The boundary condition for the finite element analysis.

3. RESULTS AND DISCUSSION

3.1. Force-Displacement Curves

Figures 5(a), (b), and (c) show the force and displacement curves of non-folded (180°) and pre-folded columns for triangular, square, and hexagonal shapes, respectively. For the non-folded thin-walled column specimen, the force quickly increases with the deformation until reaching the maximum force before fracture. The buckling effect is dominant in this case. From this curve, the thin-walled column is confirmed as a brittle material because it fails at a small deformation value with a small portion of the plastic deformation region. However, when the pre-folded pattern is introduced, significant changes for the maximum deformation (deformation value at failure) are found. On the other hand, the force does not increase as quickly as the non-folded one; it increases slowly until it reaches the maximum force at a smaller pre-folded angle. Considering the angle range from 180 to 140° , the deformation at failure for

triangular, square, and hexagonal shapes column increases by 113.7; 115; and 35.3%, respectively.

From Figure 5, the cross-section's shape influences the maximum force that occurred for each angle significantly. The hexagonal shape exhibits the highest maximum force compared with the other shapes. Then, in general, the maximum force tends to drop as the pre-folded angle changes from 180 to 140° . However, the hexagonal shape exhibits a more significant drop compared with that of the triangular and square shapes. This indicates that the shape with a lower number of edges tends to give a lower structural stiffness. The deformation of the hexagonal shape structure could not increase significantly due to the higher stiffness. In other words, more edges in cross-section shape may cause the force required to collapsing the column to become higher. This column behavior shows agreement with several works conducted by other researchers.

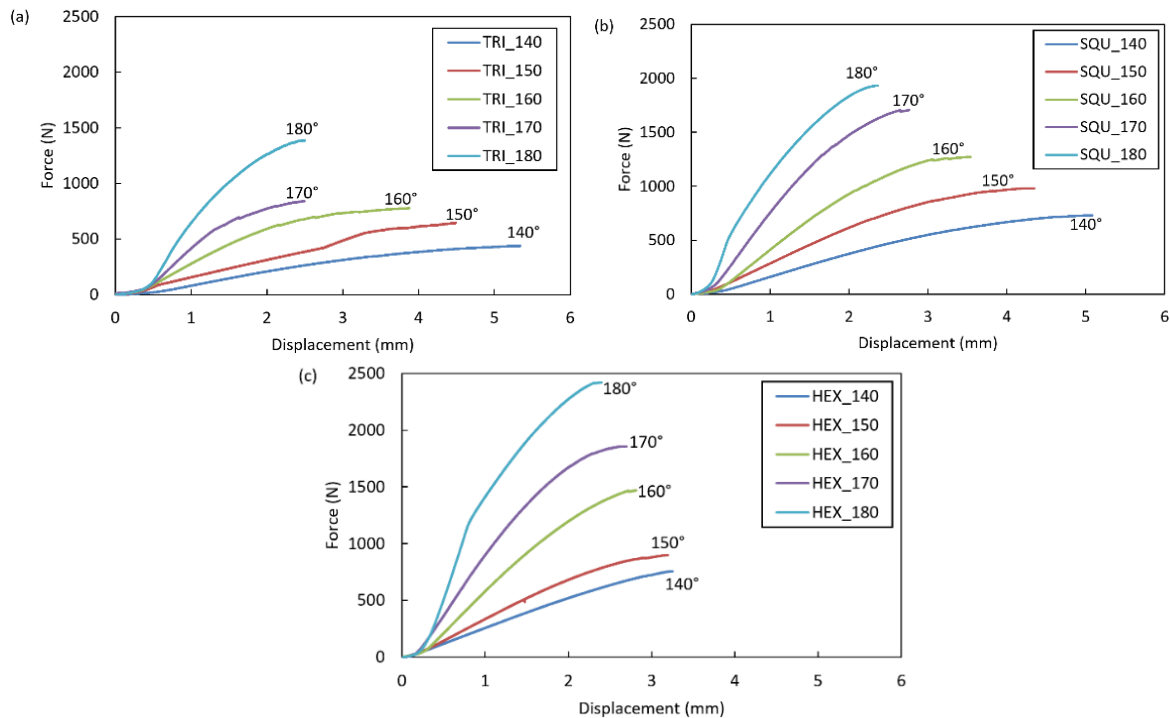


Figure 5. Force-displacement curves from compression test for different angles: (a) triangular, (b) square, (c) hexagonal patterns.

When the cross-section shape has a higher number of edges, approaching the circular shape, the maximum force increased (Goel, 2015; Liu, 2008). Considering the maximum force values, all experimental data shows a consistent tendency in which the bigger pre-folded angle causes high maximum force. These results reveal that the cross-section shape and pre-folded angle can be utilized to design the mechanical behavior of a thin-walled column as required in any engineering application.

3.2. Compressive Mechanical Behavior: Stiffness and Strength

To understand the mechanical behavior under compressive load, the structural stiffness, displacement, and strength of every specimen are analyzed and compared. The value of column stiffness was determined by analyzing the slope of the force-displacement curve for every increment of elongation. This slope plot can describe the change of tangent modulus of the structure at every strain increment. **Figure 6** shows the slope to displacement curves of all specimens. The plot shows that

the slope value increases until reaching the maximum value and then slowly decreases before failure. Based on this plot, the effective column stiffness is determined by dividing the maximum force by its corresponding displacement. The value is indicated by the maximum peak of each curve in **Figure 6**.

Figure 7 shows the calculated effective stiffness values of all specimens. The figure compares the values obtained from compression test experiments (denoted as 'Exp') and numerical simulations (denoted as 'Sim'). The experimental result plots clarify that the pre-folded pattern can effectively lower the value of structural stiffness up to 85, 82, and 77% for triangular, square, and hexagonal columns, respectively. Hence, the stiffness of a thin-walled column can be modified by introducing the pre-folded pattern and different cross-section shapes. The triangular column shows the lowest stiffness compared to the other cross-sections. This means that the triangular column is more flexible than the square and hexagonal columns. In addition, having known that a 3D printed structure made of

PLA material possesses a brittle behavior, introducing the pre-folded pattern is a technique to delay the brittle failure to occur. This is because the structure with a pre-folded pattern can endure more deformation compared with the other shapes. The possible reason for this phenomenon is that

the pre-folded pattern can distribute the deformation in the column wall. Thus, the effective stiffness of the column decreases. The detailed deformation behavior of the wall can be observed in the finite element simulation result.

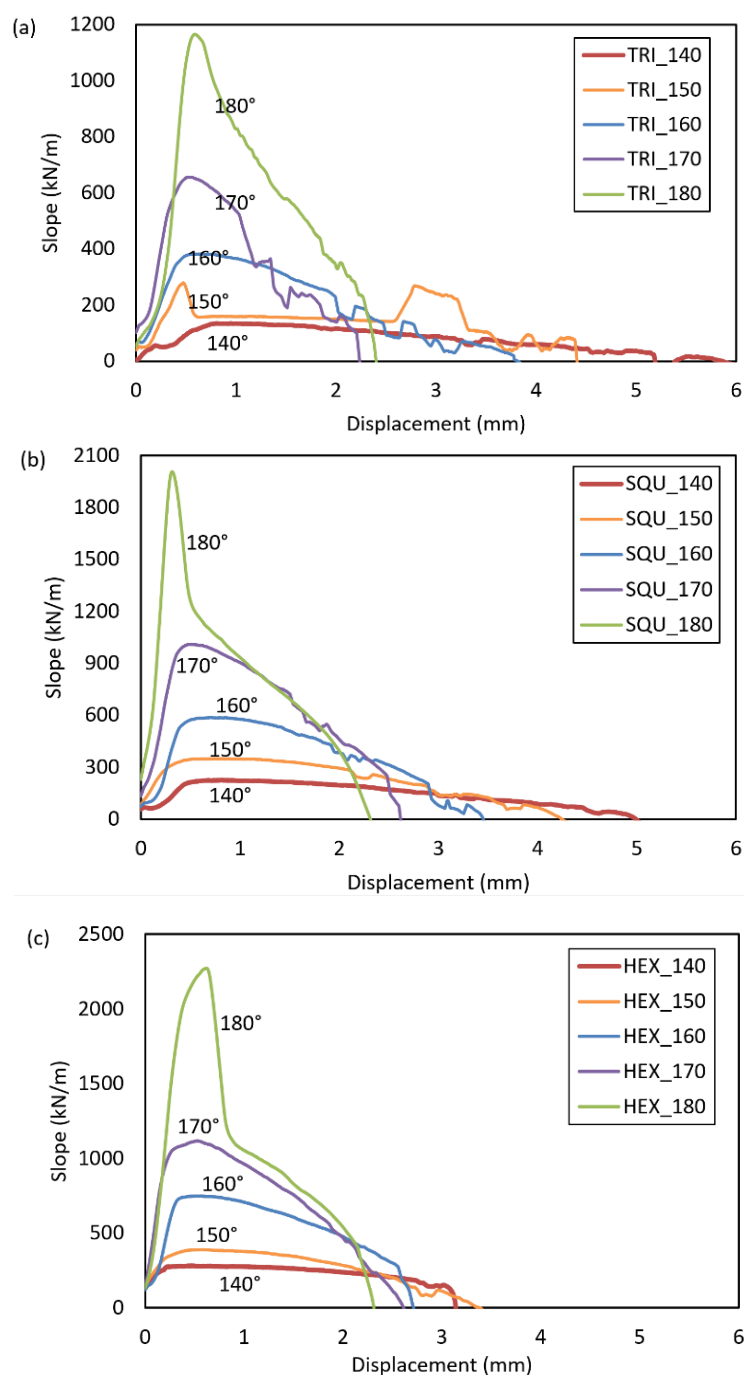


Figure 6. The slope to displacement curves for all cross-section shapes, (a) Triangular, (b) Square (c) Hexagonal, with the different pre-folded angles from 140 to 180°.

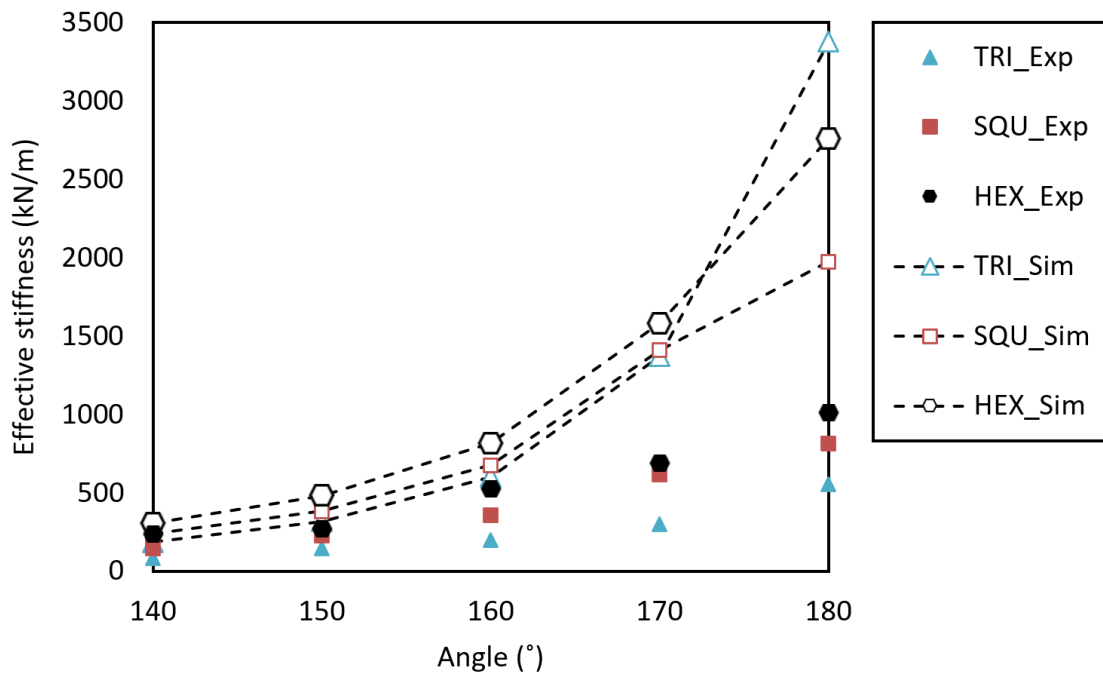


Figure 7. Structural column stiffness of pre-folded thin-walled columns obtained from compression tests (denoted as 'Exp') and numerical simulations (Sim).

The trend of effective stiffness and pre-folded angle found in the experiment is in good agreement with that obtained from the FEA. Both experiment and simulation confirm that as the pre-folded angle becomes smaller, the effective stiffness also decreases. However, the smaller angle shows closer agreement in terms of the stiffness values than that of the bigger angle. The gap of stiffness values between experiment and simulation becomes larger as the pre-folded angle approaches 180° (see **Figure 7**). The reason for this gap is possibly caused by the non-linear deformation effect, such as localized bending deformation which might be generated in the wall. In experimental results, As the angle approaches 180°, the possibility of the column's wall to experience buckling deformation will be bigger. This is considered as the instability condition due to the slenderness effect on the thin wall ([Triawan et al., 2012](#); [Triawan et al., 2018](#)). When the pre-folded angle is small (i.e., 140°), the effect of buckling deformation on the effective stiffness gradually vanishes, thus the simulation and experimental results show a good match. Note that this buckling effect is not considered in the simulation.

The normalized values of maximum displacement plotted against the pre-folded angle are shown in **Figure 8**. The maximum displacement at the failure of every specimen is normalized by the maximum displacement value of the 170° specimen. The experimental results are denoted by 'Exp', while the FEA results are denoted by 'Sim' in the graph. From these plots, it can be verified that the instability effect due to buckling deformation in the experimental result strongly affects the column specimen's deformation behavior. For the specimens with pre-folded angle, the plots from the simulation match well with the experiment, especially the hexagonal shape. However, the value drastically changes for the non-folded specimen. The simulation results show the wrong tendency of the maximum deformation measured in the experiment. The simulation results exhibit a normalized deformation of more than 1, while the experiment result showed the opposite. This is possibly caused by the buckling effect that is not considered in the simulation. Thus, the failure displacement does not reflect the actual condition.

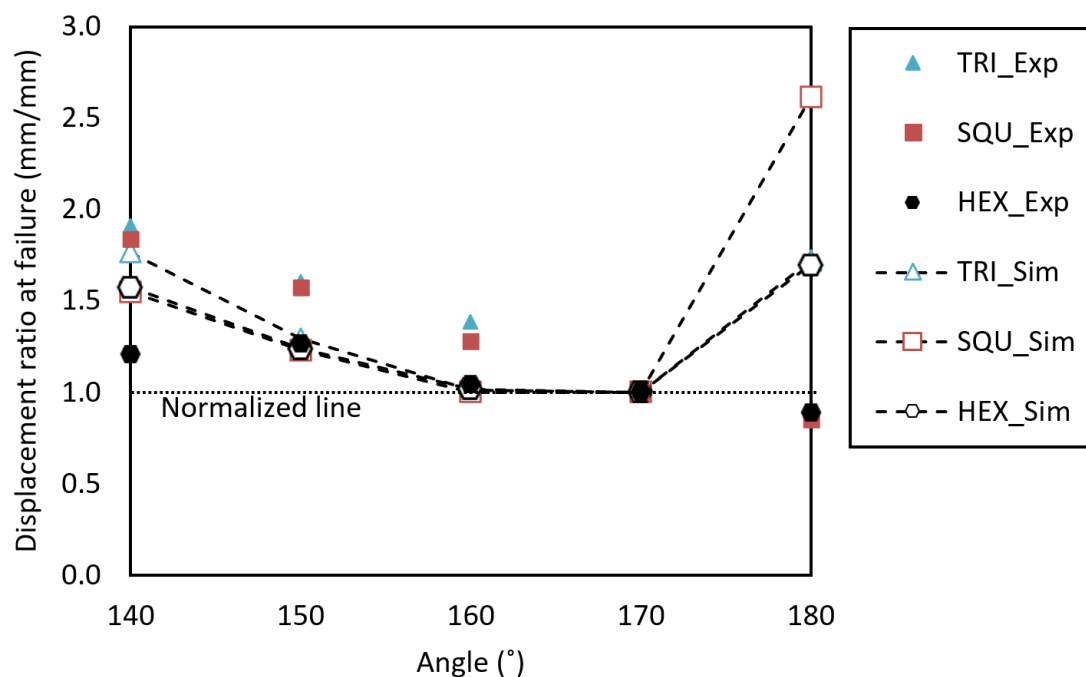


Figure 8. Deformability of non-folded and pre-folded thin-walled columns.

Figure 9 shows the typical stress distribution for the maximum principal stress (σ_1) occurred inside the structure during simulation for column model of hexagonal shape without pre-folded pattern and with 160° pre-folded angle. The location that would possibly fail is indicated by the red color in which the stress value has exceeded the tensile strength of PLA material. As the deformation increases, the stress value increases until reaching the tensile strength value. Then, failure (crack) would be initiated. For the non-folded column (see **Figure 9(a)**), the stress distribution has fluctuated along the surface. The maximum principal stress is significantly low because the buckling effect is not considered. Moreover, the pre-folded column (see **Figure 9(b)**) exhibited a more distributed stress on the whole body at the edge of the pre-folded pattern. This indicates that the pre-folded pattern is effective in avoiding the instability condition.

The values of the compressive strengths of all column specimens are plotted in **Figure 10**. The non-folded thin-walled column is indicated by 180° angle. As the pre-folded angle is introduced, the ultimate compressive strength can be modified into a lower value. This is again confirmed the benefit of utilizing pre-folded pattern with different cross-section shape in designing and controlling the mechanical behavior of thin-walled column. Similar to the stiffness and deformation, the strength values obtained from the experiment also match the trend from the simulation. However, when the angle is dismissed, the simulation results cannot properly predict the strength from the experiments. This is caused by the inclusion of non-linear deformation effect in the simulation while it does not consider the buckling effect of column wall which occurs in the experiment.

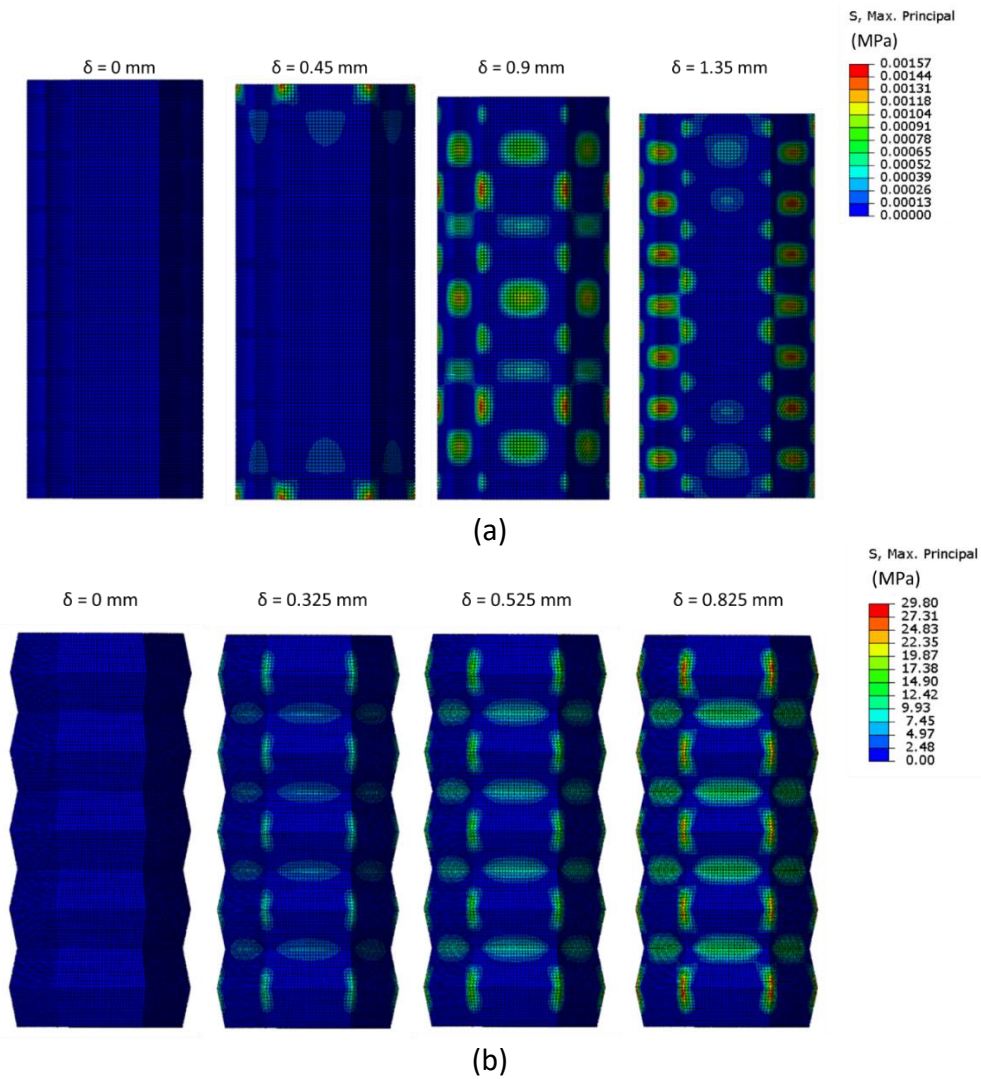


Figure 9. Stress distribution in column model under compression static simulation for case of hexagonal shape, (a) without folding angle, and (b) with the folding angle of 160° .

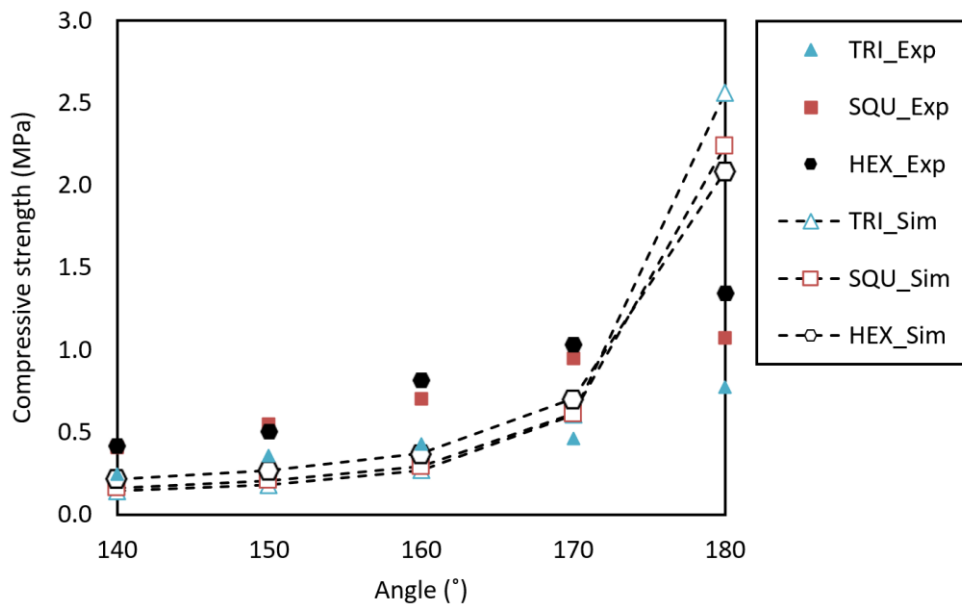


Figure 10. Compressive strength of non-folded and pre-folded thin-walled columns.

3.3. Comparison of Experiment and FEA results at the Fracture point

Since the thin-walled columns were made of Polylactic Acid (PLA) material, thus the fracture mode of the 3D printed column specimens is in a brittle fracture mode. For the non-folded column, the brittle failure mode caused the specimen to have a random fracture shape. However, after introducing the pre-folding angle pattern into the structure, the fracture shape becomes in regular shape. **Figure 11** compares the fracture shapes of the non-folded and pre-folded thin-walled column from experiment and simulation. The non-folded and pre-folded thin-walled columns show a different fracture shape. The non-folded pattern collapses with a random (irregular) shape. Meanwhile, the pre-folded pattern collapses with an almost similar fracture model to that of the simulation.

For the triangular shape shown in **Figure 11(a)**, by introducing a pre-folded pattern, the fracture tends to occur in the outer edge and inner edge of the structure. This matches with the simulation result in which the stress concentration is generated at the folding edge. According to the stress distribution from the simulation result, a similar location of cracks was found in the experiment where the stress concentration is generated. The crack could be initiated from the vertical axis at the outer edge and then is spread into the inner edge. For the square shape in **Figure 11(b)**, the stress is concentrated at the outer edge of the vertical axis as well as at the inner edge at the horizontal axis. The simulation result shows good agreement with the fracture shape from the experiment. Finally, the hexagonal-shaped column in **Figure 11(c)** also shows a similar high-stress

concentration location at the inner and outer edges from where the crack could be initiated and then propagated.

Introducing the pre-folding pattern to the thin-walled column made of PLA, which is a brittle material, can improve the structure's deformability and control the fracture mode shape. The pre-folding pattern could lead the thin-walled column to deform following its folding pattern, hence the stress concentration is distributed evenly in a certain position of the body. This is the reason why the non-folded specimen shows a very random fracture shape. As the compressive load is applied, the stress concentration is generated at a random position where some imperfections by the 3D printing process may be present (Jin *et al.*, 2020). Imperfection is considered as the weakest part of the structure. If the instability condition is achieved, the column could fail at any moment with a random shape. Meanwhile, the pre-folded pattern can be utilized to avoid this unpredictable failure, since the thin-walled column could perform a more stable and predictable deformation.

Another possible reason why a pre-folded thin-walled column can undergo longer strain compared to the non-folded one is due to an increase in the number of fold and plastic hinges in the structure during compression loading. In the 3D printing process, it is unavoidable that the thickness of the meeting edges or walls will be much thicker. As the angle decreases, the thickness of the meeting edges would be much thicker. This part can cause the structure to be able to withstand more stress. Thus, introducing the folding pattern in the thin-walled column can endure more deformation compared to the non-folded thin-walled column.

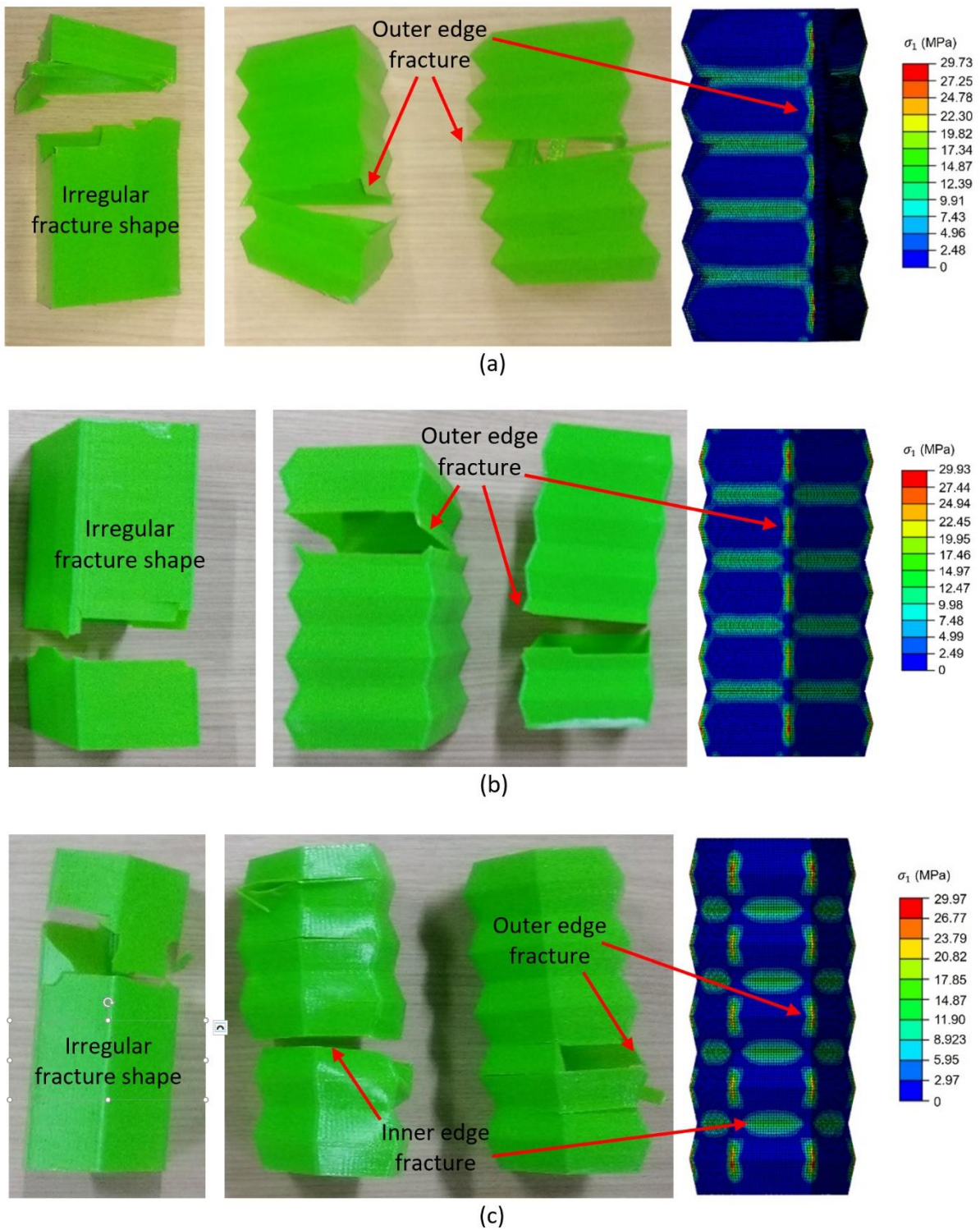


Figure 11. Fracture shape of non-folded and pre-folded (a) triangular, (b) square, and (c) hexagonal thin-walled column specimens.

Based on the comparison between the experiment and simulation results, it can be understood that the usage of the 3D printing method for fabricating any complex structures is quite reliable. The imperfection generated during the FDM 3D printing process could be made less effective in deviating the mechanical behavior by introducing the pre-folded pattern. Furthermore, the design optimization of the column to find the best pre-folded angle and cross-section shape needs to be done while keeping a reasonable low mass of the column. The design optimization result will be reported in the next article.

4. CONCLUSION

Investigation on the compressive behavior of thin-walled columns made of PLA materials and fabricated by FDM 3D Printing has been carried out by experiment and numerical simulation. The column specimens are designed with three different cross-sections (i.e., Triangular, Square, and Hexagonal shapes) and five pre-folded patterns with angles of 140, 150, 160, 170, and 180° (the non-folded column) to understand the variation of the mechanical behavior under compressive load. From the tests, the force and displacement curves are obtained to analyze the stiffness, strength, and overall deformation. As a result, the columns with non-folded patterns demonstrate the brittle failure behavior with random fracture shapes. However, after introducing the pre-folded patterns with different angles, the stiffness can be manipulated, and therefore the deformability could be increased. It is revealed that the pre-folding pattern can decrease the structural stiffness by 85% and increase the deformability by 115%, and at

the same time lower down the column strength by 68.7%. The same phenomena are also confirmed by the finite element simulation in which the non-linear effect (NLGEOM) is considered. Based on the finite element simulation, the column models with pre-folded patterns exhibit a more stable deformation behavior indicated by the uniformly distributed high-stress values in the whole column body. This allows the modification of the mechanical behavior as needed by the target application. The pre-folded thin-walled columns can experience longer strain than the non-folded columns due to the increased number of localized plastic deformation. A higher number of folding edges will result in uniform stress distribution and therefore can withstand more load. In addition, this investigation also suggests that FDM 3D Printing can be considered as a reliable fabrication process for a structure with a complex shape made of brittle material. By utilizing the flexibility of 3D printing technology, any engineering structure can be designed to have unique mechanical behavior that meets the design requirements.

5. ACKNOWLEDGMENTS

The authors express deep gratitude to the LPDP research grant, No. PRJ-85/LPDP/2020, and CRCS of Sampoerna University for providing generous funding for running this research.

6. AUTHORS' NOTE

The authors declare that there is no conflict of interest regarding the publication of this article. The authors confirmed that the paper was free of plagiarism.

7. REFERENCES

- Al-Kaseasbeh, Q., and Mamaghani, I. H. (2019). Thin-walled steel tubular circular columns with uniform and graded thickness under bidirectional cyclic loading. *Thin-Walled Structures*, 145, 106449.
- Castiblanco, P. A., Ramirez, J. L., and Rubiano, A. Smart Materials and Their Application in Robotic Hand Systems: A State of the Art. *Indonesian Journal of Science and Technology*, 6(2), 401-426.
- Chen, Z., Wu, T., Nian, G., Shan, Y., Liang, X., Jiang, H., and Qu, S. (2019). Ron Resch origami pattern inspired energy absorption structures. *Journal of Applied Mechanics*, 86(1), 011005.
- Daneshi, G. H., and Hosseinipour, S. J. (2002). Grooves effect on crashworthiness characteristics of thin-walled tubes under axial compression. *Materials and Design*, 23(7), 611-617.
- Gholipour, G., Zhang, C., and Mousavi, A. A. (2018). Effects of axial load on nonlinear response of RC columns subjected to lateral impact load: Ship-pier collision. *Engineering Failure Analysis*, 91, 397-418.
- Goel, M. D. (2015). Deformation, energy absorption and crushing behavior of single-, double- and multi-wall foam filled square and circular tubes. *Thin-walled Structures*, 90, 1-11.
- Hadisujoto, B., and Wijaya, R. (2021). Development and Accuracy Test of a Fused Deposition Modeling (FDM) 3D Printing using H-Bot Mechanism. *Indonesian Journal of Computing, Engineering and Design (IJoCED)*, 3(1), 46-53.
- Han, D. C., and Park, S. H. (1999). Collapse behavior of square thin-walled columns subjected to oblique loads. *Thin-Walled Structures*, 35(3), 167-184.
- Ishida, S., Suzuki, K., and Shimosaka, H. (2017). Design and experimental analysis of origami-inspired vibration isolator with quasi-zero-stiffness characteristic. *Journal of Vibration and Acoustics*, 139(5), 051004.
- Jin, Z., Zhang, Z., and Gu, G. X. (2020). Automated real-time detection and prediction of interlayer imperfections in additive manufacturing processes using artificial intelligence. *Advanced Intelligent Systems*, 2(1), 1900130.
- Kuribayashi, K., Tsuchiya, K., You, Z., Tomus, D., Umemoto, M., Ito, T., and Sasaki, M. (2006). Self-deployable origami stent grafts as a biomedical application of Ni-rich TiNi shape memory alloy foil. *Materials Science and Engineering: A*, 419(1-2), 131-137.
- Lee, S., Hahn, C., Rhee, M., and Oh, J. E. (1999). Effect of triggering on the energy absorption capacity of axially compressed aluminum tubes. *Materials and Design*, 20(1), 31-40.
- Liu, Y. (2008). Crashworthiness design of multi-corner thin-walled columns. *Thin-Walled Structures*, 46(12), 1329-1337.
- Ma, J. Y., and You, Z. (2014a). Energy absorption of thin-walled beams with a pre-folded origami pattern. *Applied Mechanics and Materials*, 566, 569-574.
- Ma, J. Y., and You, Z. (2014b). Energy absorption of thin-walled beams with a pre-folded origami pattern. *Applied Mechanics and Materials*, 566(1), 569-574.

- Ma, J., Dai, H., Shi, M., Yuan, L., Chen, Y., and You, Z. (2019). Quasi-static axial crushing of hexagonal origami crash boxes as energy absorption devices. *Mechanical Sciences*, 10(1), 133–143.
- Moon, S. K., Tan, Y. E., Hwang, J., and Yoon, Y. J. (2014). Application of 3D printing technology for designing light-weight unmanned aerial vehicle wing structures. *International Journal of Precision Engineering and Manufacturing - Green Technology*, 1(3), 223–228.
- Nia, A. A., and Hamedani, J. H. (2010). Comparative analysis of energy absorption and deformations of thin walled tubes with various section geometries. *Thin-Walled Structures*, 48(12), 946–954.
- Nikoo, H. M., Bi, K., and Hao, H. (2020). Textured pipe-in-pipe system: A compound passive technique for vortex-induced vibration control. *Applied Ocean Research*, 95, 102044.
- Reid, S. R. (1993). Plastic deformation mechanisms in axially compressed metal tubes used as impact energy absorbers. *International Journal of Mechanical Sciences*, 35(12), 1035–1052.
- Rismalia, M., Hidajat, S. C., Permana, I. G. R., Hadisujoto, B., Muslimin, M., and Triawan, F. (2019). Infill pattern and density effects on the tensile properties of 3D printed PLA material. *Journal of Physics: Conference Series*, 1402(4), 44041.
- Sadeghi, S., and Li, S. (2019). Fluidic origami cellular structure with asymmetric quasi-zero stiffness for low-frequency vibration isolation. *Smart Materials and Structures*, 28(6), 65006.
- Singace, A. A., and El-Sobky, H. (1997). Behaviour of axially crushed corrugated tubes. *International Journal of Mechanical Sciences*, 39(3), 249–261.
- Triawan, F., Budiman, B. A., Juangsa, F. B., Prananto, L. A., and Aziz, M. (2018). Finite element analysis on the unloading elastic modulus of aluminum foams by unit-cell model. *IOP Conference Series: Materials Science and Engineering*, 288(1), 012069.
- Triawan, F., Denatra, G. C., and Djamari, D. W. (2020). Quasi-static compressive properties and behavior of single-cell miura origami column fabricated by 3D printed PLA material. *International Journal of Sustainable Transportation Technology*, 3(2), 66-73.
- Triawan, F., Kishimoto, K., Adachi, T., Inaba, K., Nakamura, T., and Hashimura, T. (2012). The elastic behavior of aluminum alloy foam under uniaxial loading and bending conditions. *Acta Materialia*, 60(6–7), 3084–3093.
- Wang, T., Zhang, L., Zhao, H., and Chen, Q. (2016). Progressive collapse resistance of reinforced-concrete frames with specially shaped columns under loss of a corner column. *Magazine of Concrete Research*, 68(9), 435–449.
- Yang, K., Xu, S., Shen, J., Zhou, S., and Xie, Y. M. (2016). Energy absorption of thin-walled tubes with pre-folded origami patterns: Numerical simulation and experimental verification. *Thin-Walled Structures*, 103, 33–44.
- Yang, K., Xu, S., Zhou, S., and Xie, Y. M. (2018). Multi-objective optimization of multi-cell tubes with origami patterns for energy absorption. *Thin-Walled Structures*, 123, 100–113.

Yu, M., Yang, W., Yu, Y., Cheng, X., and Jiao, Z. (2020). A crawling soft robot driven by pneumatic foldable actuators based on Miura-ori. *Actuators*, 9(2), 26.

Zhou, J., Dong, C., Chen, B., and Niu, X. (2021). Design and numerical simulation of pyramidal prefolded patterned thin-walled tubes. *Advances in Materials Science and Engineering*, 2021, 1-16.